

Holographic shaping of generalized self-reconstructing light beams

Laura C. Thomson and Johannes Courtial

*Department of Physics & Astronomy, University of Glasgow, Glasgow G12 8QQ,
United Kingdom*

Abstract

Bessel beams are an example of self-reconstructing (or self-healing) light beams. This property is useful in optical tweezers. Here we modify the Curtis-Koss-Grier algorithm [J. E. Curtis *et al.*, Opt. Commun. **207**, 169 (2002)], which is frequently used in optical tweezers, to utilize the Fourier-space properties of such light beams for the construction of arbitrary self-reconstructing light beams. We demonstrate the performance of this algorithm using numerical simulations.

Key words: Computer holography, Laser beam shaping, Optical tweezers

PACS: 090.1760, 140.3300, 999.9999

1 Introduction

Due to their self-reconstructing character, Bessel beams are interesting for optical trapping of 3-dimensional structures [1,2]. On propagation, the shadow of any object placed in the beam splits into different parts, which move away from the shadow core. Therefore the part of the beam directly behind the object is reconstructed to what it would have been without the obstruction [3–5].

In addition to being self-reconstructing, Bessel beams are propagation-invariant over a relatively long distance. Unlike Gaussian beams, they do not possess a focus but a bright line or cylinder centred on the beam axis. It is also possible to shape the transverse cross-section of non-diffracting beams into regular [6], arbitrary [7], or random [8] patterns, and the full three-dimensional intensity

Email address: j.courtial@physics.gla.ac.uk (Laura C. Thomson and Johannes Courtial).

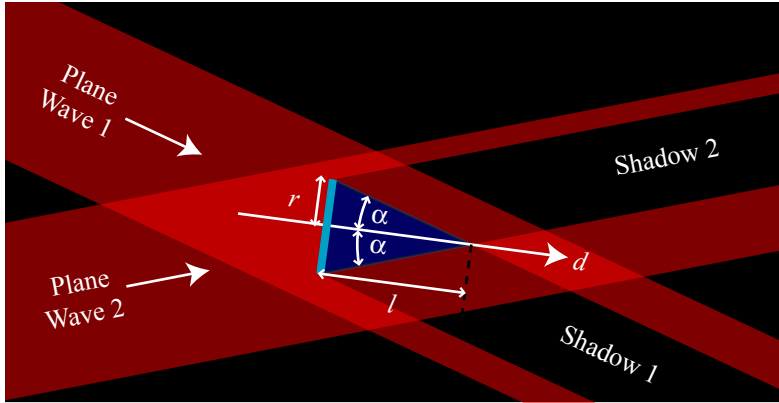


Fig. 1. Example of self-reconstruction of a light beam behind a particle of radius r (thick light blue line). The light beam consists of two plane waves (red), respectively travelling at angles of $\pm\alpha$ with respect to the self-reconstruction direction, \mathbf{d} . The particle creates a shadow in each plane wave; their overlap forms the core shadow (dark blue) of length l . In other words, a distance l behind the particle all plane waves are overlapping again, hence the beam is reconstructed.

distribution into the corresponding elongated pattern. (References [6–8] used computer-controlled phase holograms in the form of spatial light modulators (SLMs).) As the three-dimensional intensity distribution defines the trapping potential – for dielectric particles, the bright regions define the shape of the trap –, a Bessel beam corresponds to a very elongated trap. This is useful for optical guiding, but not usually desirable in optical trapping.

Superpositions of Bessel beams are as self-reconstructing as their individual Bessel-beam components, and they can change on propagation. Simple superpositions of Bessel beams have already been used to create very specific, non-propagation-invariant, trap configurations such as conveyor belts [2].

Here we extend the concept of self-reconstructing light beams. We restrict ourselves to monochromatic beams of wavelength λ ; generalization to polychromatic light beams is straightforward. In Bessel beams, all plane-wave components in the beam are inclined with respect to the propagation direction by the *same* angle [9]; in generalized self-reconstructing beams, all plane-wave components are inclined with respect to the direction \mathbf{d} in which the beam is propagation-invariant by a *minimum* angle, α . As before, any shadow due to an obstruction in the beam centre moves outwards on propagation in the \mathbf{d} direction, allowing the outside of the beam to reconstruct the centre (figure 1). Such beams can be propagation-invariant, but they do not have to be. Specifically, they can contain many intensity maxima in arbitrary 3D positions, each of which tightly constrained in all directions and therefore well suited for many optical-trapping applications.

The Fourier-space representation of a monochromatic light beam is zero everywhere apart from the surface of a sphere of radius $k = 2\pi/\lambda$ (the Ewald

sphere). Different points on the sphere correspond to plane-wave components travelling in different directions. The absence of light travelling within an angle α of the \mathbf{d} direction in generalized self-reconstructing beams corresponds to a dark disc on the Ewald sphere, centred around the point corresponding to the \mathbf{d} direction. We exploit this Fourier-space property of self-reconstructing beams by using a well-known beam-shaping algorithm to reconcile approximately the desired intensity structure of the beam with the Fourier-space constraints of generalized self-reconstructing beams, thereby creating an algorithm for shaping generalized self-reconstructing beams. By creating other dark areas in the plane-wave spectrum we can create beams that self-reconstructing in a number of directions simultaneously.

2 Algorithm for shaping generalised self-reconstructing beams

We use a modification of the Curtis-Koss-Grier algorithm [10], an iterative algorithm that allows the creation of arbitrary 3D arrangements of bright spots. Many details are not important here and can be found in Ref. [10].

What is important for our purposes is that the algorithm allows the power distribution on the Ewald sphere to be specified: the distribution of the illumination intensity in the hologram plane is a parallel projection of the power distribution on the Ewald sphere into the k_x - k_y plane, and this illumination-intensity distribution is directly specified (see figure 2). By specifying the beam illuminating the hologram to have dark discs, we can therefore make any beam produced by the hologram self-reconstructing. As can be seen from figure 2, the radius of the dark disc in the hologram illumination, ρ , is related to the angle α through the equation

$$\tan \alpha = \frac{\rho}{f}, \quad (1)$$

where f is the focal length of the Fourier lens (or the effective focal length of any combination of lenses between the hologram and the Fourier plane).

3 Examples of shaped generalised self-reconstructing beams

We numerically demonstrate the self-reconstruction of light beams shaped by our algorithm in a particularly simple situation: two traps positioned one behind the other with a separation of variable distance Δz (figure 2). In our model, the first trap contains a particle whose effect on the beam is particularly easy to model: a completely absorbing circular disc (variable radius r) in the

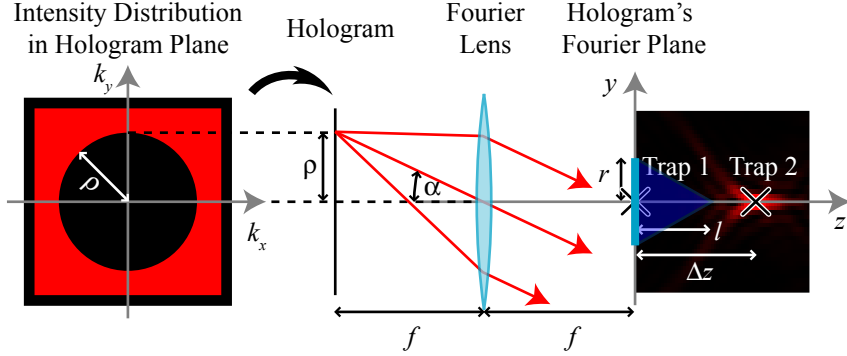


Fig. 2. Schematic of part of a set-up for self-reconstructing Fourier holography. The hologram directly defines the k -space structure of the beam behind the Fourier lens (focal length f); a centred dark region of radius ρ in the hologram-illumination intensity (red = bright, black = dark) defines a dark region in k space. The light rays (red) are drawn for a point at the edge of the dark region. They represent light rays inclined at the minimum inclination angle, α . Self reconstruction of beams containing two traps, with a particle of radius r held in trap 1 and throwing a core shadow of length l , are discussed in section 3.

transverse plane. The particle trapped in our model does not exhibit any refraction effects, which can lead to optical binding [11]. We simulate wave-optically the beam propagation behind the trapped particle – and therefore the shadow cast by it – and investigate the effect the shadow has on the formation of the second trap.

Figure 3 shows yz ($x = 0$) intensity cross-sections in a light beam with two traps separated longitudinally. Different frames are calculated for different particle radii, representing the light beam with respectively no obstruction; an obstruction that throws a core shadow shorter than the trap separation; and an obstruction with a core shadow that covers the position of trap 2. As expected, in the first two cases trap 2 is fully (re)constructed; in the third case it is not.

We investigate the transition of full reconstruction to virtually complete extinction in more detail. We define the critical radius, R , as the particle radius for which the length of the particle's shadow, l , equals the trap separation, Δz . As the length l of the core shadow behind a particle of radius r is given by the equation

$$\tan \alpha = \frac{r}{l} \quad (2)$$

(see figure 1), the critical radius is given by

$$\tan \alpha = \frac{R}{\Delta z}. \quad (3)$$

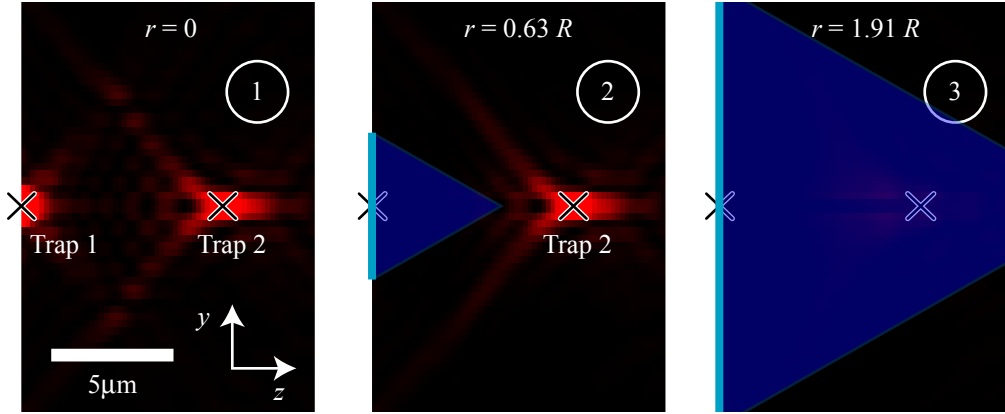


Fig. 3. Intensity cross-sections in the yz ($x = 0$) plane as the radius, r , of a particle trapped in trap 1 is varied. The particle radius is given in multiples of the critical radius, R , which is $4.69\mu\text{m}$ for the trap separation we use here, $\Delta z = 8.25\mu\text{m}$. The particle is shown as a thick light blue line, its core shadow is shown in dark blue. Cases 1 to 3 show the light beam respectively for particle radius 0, with both traps fully developed; for non-zero, but less than the critical, particle radius, with the second trap fully developed ($r = 0.63R$); and for a particle radius greater than the critical radius, with the second trap lying in the core shadow and therefore destroyed ($r = 1.91R$). Like all the other results shown in this section, this figure was calculated for a hologram of size $20\text{mm} \times 20\text{mm}$, which was uniformly illuminated outside the dark disc of radius $\rho = 6.25\text{mm}$. We simulated this on a grid of 256×256 points for light of wavelength $\lambda = 633\text{nm}$; the effective focal length was $f = 11\text{mm}$ (which is representative of the Glasgow tweezers experiment [12]).

The three frames in figure 3 actually represent the cases $r = 0$, $r < R$, and $r > R$.

Figure 4 shows the intensity at the position of trap 2, I_2 , plotted as a function of r/R for constant values of Δz and α . As the particle radius is increased from 0 to the critical radius ($0 < r/R < 1$), the intensity in trap 2, I_2 , remains approximately constant (with ripples of the same origin as those shown in figure 3 in Ref. [9]); ray-optically, the shadow cast by the trapped particle is shorter than the trap separation Δz and hence the second trap is fully reconstructed. As r/R is increased further ($r/R > 1$), the intensity in trap 2 begins to decrease; ray-optically, the trapped particle begins to cast a shadow over the second trap, hence the second trap is not fully reconstructed.

We also investigate a situation in which the particle radius is fixed and the trap separation Δz is varied. Now there is a critical trap separation Z equal to the length l of the shadow cast by the trapped particle, given by

$$\tan \alpha = \frac{r}{Z}. \quad (4)$$

Figure 5 shows the intensity at the position of trap 2, I_2 , as a function of $\Delta z/Z$.

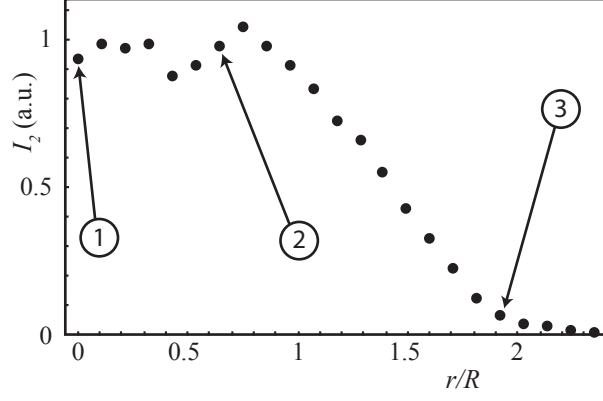


Fig. 4. Intensity in trap 2, I_2 , in a beam with a fixed trap separation, plotted as a function of the particle radius, r , in multiples of the critical radius, R . yz intensity cross-sections corresponding to points 1, 2 and 3 are shown in figure 3. Beam and simulation parameters like in figure 3.

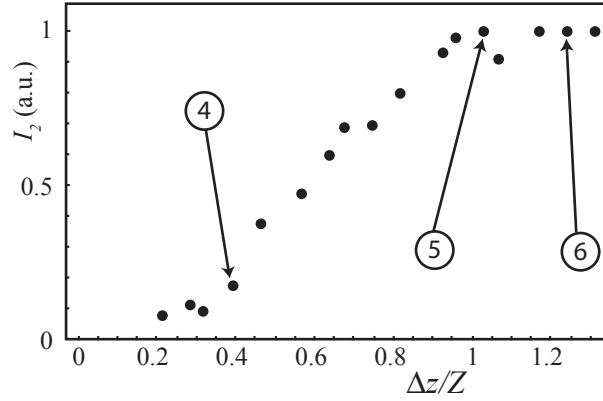


Fig. 5. Intensity in trap 2, I_2 , plotted for beams with different trap separations, Δz . A particle of fixed radius $r = 3\mu\text{m}$ is trapped in trap 1. Δz is given in multiples of the critical trap separation, Z ; remaining beam and simulation parameters are the same as in figure 3. yz intensity cross-sections corresponding to points 4, 5, and 6 are shown in figure 6. Note that the data points are more noisy than those in figure 4; a new hologram had to be calculated for each data point in this graph (and this involves iterative processes, which can arrive at completely different holograms for only slightly different target intensity distributions), whereas all data points in figure 4 were calculated for the same hologram.

As expected, I_2 rises from close to zero to a near-constant value as trap 2 is moved away from trap 1 and out of the shadow of the particle trapped there. Figure 6 shows yz intensity cross sections corresponding to some of the data points.

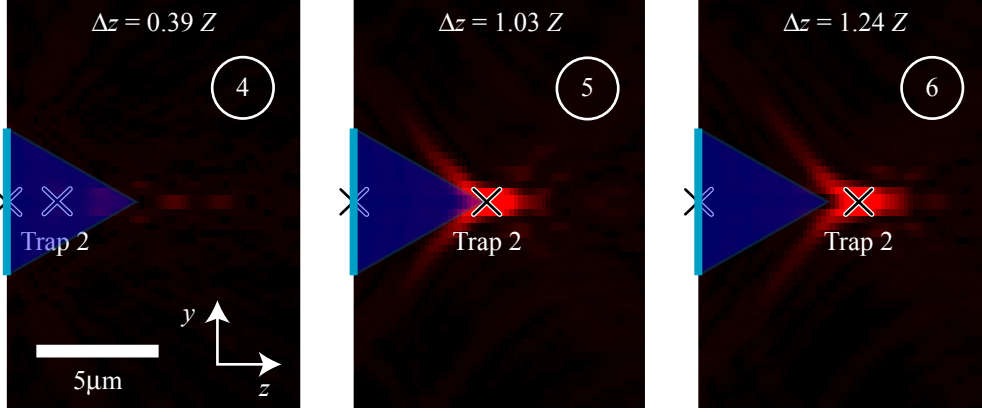


Fig. 6. yz ($x = 0$) intensity cross-sections for the same particle radius $r = 3\mu\text{m}$, but different trap separations Δz , given in multiples of the critical trap separation, Z ; remaining beam and simulation parameters are as described in the caption of figure 3. Like in figure 3, the particle is shown as a thick light blue line, its core shadow is shown in dark blue. The intensities in trap 2 corresponding to these frames are shown in figure 5.

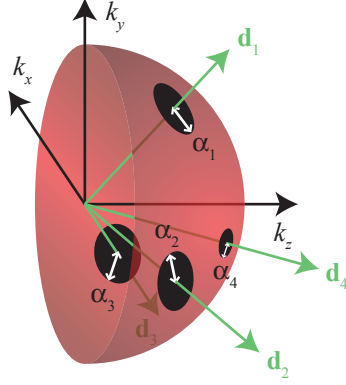


Fig. 7. k -space distribution of a monochromatic light beam that is self-reconstructing in the directions \mathbf{d}_1 to \mathbf{d}_4 . In a monochromatic beam of wavelength λ , all light is concentrated on a sphere of radius $2\pi/\lambda$ – the Ewald sphere. Dark spots around directions \mathbf{d}_i on the Ewald sphere make the light beam self-reconstructing in the direction \mathbf{d}_i , whereby the reconstruction distance behind an obstruction is given by the angular radius of the dark spot, α_i , and the radius of the obstruction.

4 Light beams that self-reconstruct in directions other than the propagation direction

Here we briefly discuss a generalization of self-reconstructing beams that might be useful for applications such as the trapping of photonic crystal structures [13].

It is possible to create light beams that are self-reconstructing in a direction other than the propagation direction and even in multiple directions. A light beam is self-reconstructing in any direction \mathbf{d}_i around which its k -space rep-

resentation is dark (Fig. 7). As before, the self-reconstruction distance in a particular direction \mathbf{d}_i is given by the angular radius α_i of the corresponding dark spot in k space, which is simply the minimum angle with which plane waves are inclined with respect to the direction \mathbf{d}_i . The length l of the core shadow in the direction \mathbf{d}_i corresponding to an obstruction of radius r can then be calculated from equation (2) with $\alpha = \alpha_i$.

This can be used to engineer light beams that are self-reconstructing in arbitrarily many, arbitrarily chosen, directions, whereby the corresponding self-reconstruction distances can be arbitrarily selected. As in section 2, all that is required is to specify in the Curtis-Koss-Grier algorithm the intensity distribution of the light beam illuminating the hologram to have dark spots of the right size in the right places.

Future work should examine this idea in more detail. In this way it should, for example, be possible to create a “light crystal” such that the light beam is self-reconstructing in all directions between nearest neighbours, which could perhaps be useful for optically assembling photonic crystals.

Summary and conclusions

Optical self-reconstruction (or self-healing) can be understood in terms of a simple ray-optical argument. We have generalized this concept to beams that are not necessarily non-diffracting, and to beams that are self-reconstructing in more than one direction. We have developed an algorithm for shaping such beams, and demonstrate it using a wave-optical simulation of a completely absorbing particle trapped in such a beam.

We believe such generalized self-reconstructing light beams will be useful in optical-tweezers experiment. Engineering the illumination in the hologram plane could also open up new directions in research on optical binding.

References

- [1] V. Garcés-Chávez, D. McGloin, H. Melville, W. Sibbett, and K. Dholakia, “Simultaneous micromanipulation in multiple planes using a self-reconstructing light beam,” *Nature* **419**, 145–147 (2002).
- [2] T. Čižmár, V. Garcés-Chávez, K. Dholakia, and P. Zemánek, “Optical conveyor belt for delivery of submicron objects,” *Appl. Phys. Lett.* **86**(17), 174101 (pages 3) (2005). URL <http://link.aip.org/link/?APL/86/174101/1>.

- [3] S. Chávez-Cerda, “A new approach to Bessel beams,” *J. Mod. Opt.* **46**, 923–930 (1999).
- [4] S. Chávez-Cerda and G. New, “Evolution of focused Hankel waves and Bessel beams,” *Opt. Commun.* **181**, 369 – 377 (2000).
- [5] M. Angulano-Morales, M. M. Méndez-Otero, M. D. Iturbe-Castillo, and S. Chávez-Cerda, “Conical dynamics of Bessel beams,” *Opt. Eng.* **46**, 078,001 (2007).
- [6] J. A. Davis, D. M. Cottrell, and E. Carcole, “Nondiffracting interference patterns generated with programmable spatial light modulators,” *Appl. Opt.* **35**, 599–602 (1996). URL <http://www.opticsinfobase.org/abstract.cfm?URI=ao-35-4-599>.
- [7] J. Courtial, G. Whyte, Z. Bouchal, and J. Wagner, “Iterative algorithms for holographic shaping of non-diffracting and self-imaging light beams,” *Opt. Express* **14**, 2108–2116 (2006). URL <http://www.opticsinfobase.org/abstract.cfm?URI=oe-14-6-2108>.
- [8] D. M. Cottrell, J. M. Craven, and J. A. Davis, “Nondiffracting random intensity patterns,” *Opt. Lett.* **32**, 298–300 (2007). URL <http://www.opticsinfobase.org/abstract.cfm?URI=ol-32-3-298>.
- [9] J. Durnin, J. J. J. Miceli, and J. H. Eberly, “Diffraction-free Beams,” *Phys. Rev. Lett.* **58**, 1499–1501 (1987).
- [10] J. E. Curtis, B. A. Koss, and D. G. Grier, “Dynamic holographic optical tweezers,” *Opt. Commun.* **207**, 169–175 (2002).
- [11] S. A. Tatarkova, A. E. Carruthers, and K. Dholakia, “One-Dimensional Optically Bound Arrays of Microscopic Particles,” *Phys. Rev. Lett.* **89**, 283,901 (2002). URL <http://link.aps.org/abstract/PRL/v89/e283901>.
- [12] J. Leach, K. Wulff, G. Sinclair, P. Jordan, J. Courtial, L. Thomson, G. Gibson, K. Karunwi, J. Cooper, Z. J. Laczik, and M. Padgett, “Interactive approach to optical tweezers control,” *Appl. Opt.* **45**, 897–903 (2006). URL <http://www.opticsinfobase.org/abstract.cfm?URI=ao-45-5-897>.
- [13] E. R. Dufresne and D. G. Grier, “Optical tweezer arrays and optical substrates created with diffractive optics,” *Rev. Scient. Instr.* **69**, 1974–1977 (1998). URL <http://link.aip.org/link/?RSI/69/1974/1>.